Thallium(I) complexes of tris(pyridyl)borates and a comparison to their pyrazolyl analogs

Mukundam Vanga,[a] Vo Quang Huy Phan,[a] Jiang Wu,[a] Alvaro Muñoz Castro,[b] H. V. Rasika Dias[a],*

[a]Department of Chemistry and Biochemistry, The University of Texas at Arlington, Arlington, Texas 76019, USA

[b]Facultad de Ingeniería, Arquitectura y Diseño, Universidad San Sebastián, Bellavista 7, Santiago, 8420524, Chile.

TOC Figure and Content

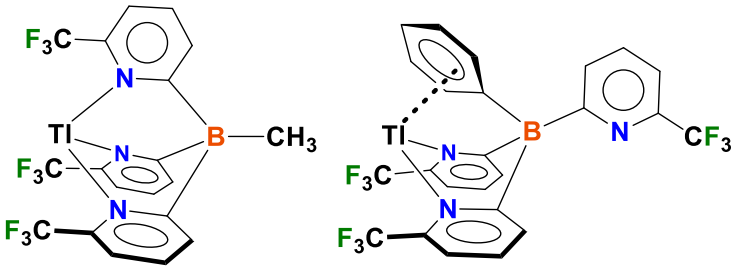

Thallium bound, fluoroalkyl-lined scorpionates based on pyridyl groups have been synthesized and compared to tris(pyrazolyl)borates with related substitution patterns.

Abstract. Thallium(I) complexes of B-methylated and B-phenylated tris(pyridyl)borates featuring trifluoromethyl groups at the pyridyl ring 6-positions have been synthesized by metathesis using the corresponding potassium salts [MeB(6-(CF$_3$)Py)$_3$]K and [PhB(6-(CF$_3$)Py)$_3$]K with thallium(I) acetate. Closely related tris(pyrazolyl)borate analog [PhB(3-(CF$_3$)Pz)$_3$]Tl has also been prepared, and comparisons of structural and spectroscopic features between the two scorpionate families are presented. The [MeB(6-(CF$_3$)Py)$_3$]Tl displays κ^3-coordination of the tris(pyridyl)borate similar to tris(pyrazolyl)borate in [MeB(3-(CF$_3$)Pz)$_3$]Tl, while [PhB(6-(CF$_3$)Py)$_3$]Tl and [PhB(3-(CF$_3$)Pz)$_3$]Tl feature κ^2-*NN* ligand coordination modes with the B-phenyl groups flanking the thallium sites. The ^{19}F NMR spectroscopy of [MeB(6-(CF$_3$)Py)$_3$]Tl reveals the presence of a remarkably large 1208 Hz four-bond thallium-fluorine coupling constant in chloroform at room temperature, which is considerably larger than 878 Hz observed for the (pyrazolyl)borate analog [MeB(3-(CF$_3$)Pz)$_3$]Tl. Although [PhB(6-(CF$_3$)Py)$_3$]Tl is structurally nonrigid at room temperature in chloroform, at lower temperatures, the ligand arm-exchange slows down revealing $^4J_{\text{Tl-F}}$ of 1110 Hz. Steric demands of these ligands have been quantified using buried volume concept. In addition, ligand transfer chemistry from [MeB(6-(CF$_3$)Py)$_3$]Tl and [PhB(6-(CF$_3$)Py)$_3$]Tl to copper(I) under ethylene, as well as computational analyses of the various coordination modes of tris(pyrazolyl)borates and tris(pyridyl)borates are reported.

Introduction.

Due to the ease of ligand assembly from common starting materials, and readily modifiable ligand steric and electronic properties through pyrazolyl ring substituents, many tris(pyrazolyl)borate ligand varieties have been synthesized and utilized as supporting ligands in metal coordination chemistry facilitating numerous applications ranging from enzyme active site modeling to catalysis.[1-8] Tris(pyrazolyl)borate ligands are commonly obtained as alkali metal salts via the reactions between pyrazoles and alkali metal borohydrides MBH_4 (M = Li, Na, K) under high temperature conditions. Although tris(pyrazolyl)borato alkali metal salts can serve as ligand transfer agents, conversion to their thallium(I) derivatives (via metathesis using thallium salts such as $TlNO_3$, TlOAc) is quite common to facilitate the separation and purification of tris(pyrazolyl)borate ligands from crude reaction mixtures, and because of their solubility in common organic solvents, ease of crystallization, and milder (less reducing) and efficient ligand transfer qualities.[4, 9-15] Direct routes to tris(pyrazolyl)boratothallium complexes from $TlBH_4$ and pyrazoles are also available.[15] Thallium complexes of tris(pyrazolyl)borates are also of interest in their own right since they display interesting NMR (Tl exists as two naturally occurring spin ½ isotopes; ^{203}Tl and ^{205}Tl) and structural (in certain cases, Tl•••Tl contacts) features.[9, 16-19]

Tris(pyridyl)borates are an emerging class of ligands.[20] They have several different features compared to the better-known tris(pyrazolyl)borates as they have B-C linkages (compared to the B-N linkages),[20] four-substitutable positions on pyridyl groups (vs three on pyrazolyl moieties), a closer proximity of the heterocyclic ring substituent (specifically, pyridyl ring 6-substient vs pyrazolyl ring 3-substient) to the metal site, and are expected to be better σ-donor ligands.[20] We recently reported the fluorinated tris(pyridyl)borate ligands including those bearing substituents at the 6-position of the pyridyl arms.[21-24] In addition to the parent tris(pyridyl)borates,[25] non-fluorinated ligands versions with alkyl and aryl substituents at the pyridyl ring 6-positions are also now known.[20, 24, 26] Recent work suggests that these are good supporting ligands for d-block metals.[20] Notably however, there are no thallium adducts of tris(pyridyl)borates in the literature to our knowledge. In contrast, closer to 100 structurally

characterized tris(pyrazolyl)boratothallium(I) complexes are in the Cambridge Structural Database (CSD),[27] which also include molecules with perfluoroalkyl substituents surrounding the thallium sites (albeit very limited in number, Figure 1).[17, 19, 28-33] In this paper, we describe the synthesis, and first structural and spectroscopic details of thallium tris(pyridyl)borates (**1** and **2**, Figure 2) and a comparison to their tris(pyrazolyl)borate analogs (**3** and **4**). In addition, coordination mode preferences were evaluated via DFT calculations.

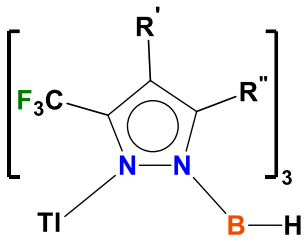

Figure 1. Structurally characterized tris(pyrazolyl)hydroborato thallium complexes with CF_3 substituents at the pyrazolyl ring 3-positions: R' = H, R" = CF_3;[28-29] R' = H, R" = thienyl;[19] R' = H, R" = Ph;[34] R' = H, R" = ferrocenyl;[17] R' = Br, R" = CF_3.[33]

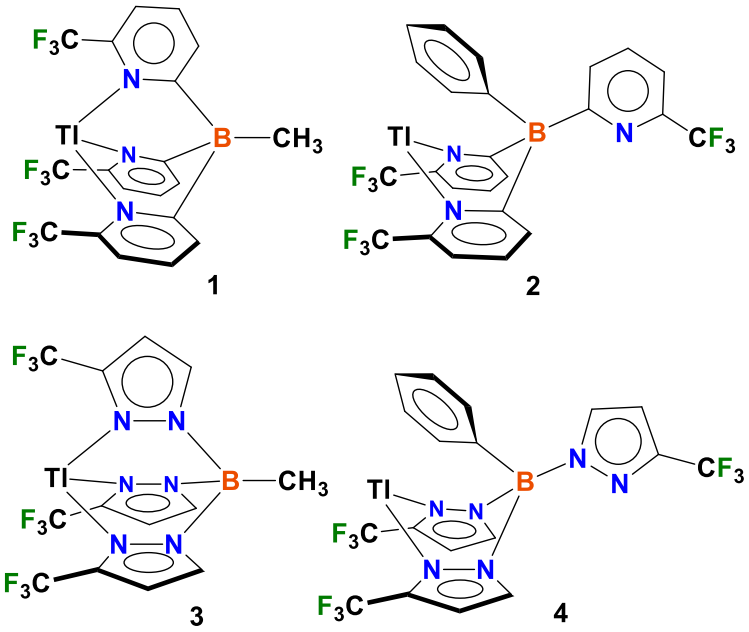

Figure 2. Structures of [MeB(6-(CF_3)Py)$_3$]Tl (**1**), [PhB(6-(CF_3)Py)$_3$]Tl (**2**), [MeB(3-(CF_3)Pz)$_3$]Tl (**3**), and [PhB(3-(CF_3)Pz)$_3$]Tl (**4**), where Py = pyridyl, Pz = pyrazolyl.

Results and discussion

The thallium complex [MeB(6-(CF_3)Py)$_3$]Tl (**1**) has been synthesized via metathesis of [MeB(6-(CF_3)Py)$_3$]K and thallium(I) acetate and isolated as a pale yellow solid in 78% yield (Scheme 1). The B-phenylated version, [PhB(6-(CF_3)Py)$_3$]Tl (**2**) was obtained via a similar process and isolated as an off-white solid in 75% yield (Scheme 1). The supporting ligand [PhB(6-(CF_3)Py)$_3$]$^-$ utilized for the latter is also new and the synthetic details and the properties of its potassium salt are provided. In addition, we have synthesized a closely related tris(pyrazolyl)borate [PhB(3-(CF_3)Pz)$_3$]Tl (**4**) using [PhB(3-(CF_3)Pz)$_3$]Li and thallium(I) acetate, for a direct comparison between **2** and **4** representing the tris(pyridyl)borate and tris(pyrazolyl)borate systems, respectively. [MeB(3-(CF_3)Pz)$_3$]Tl (**3**) which is the closest relative of **1** from the tris(pyrazolyl)borate family has been reported earlier.[30]

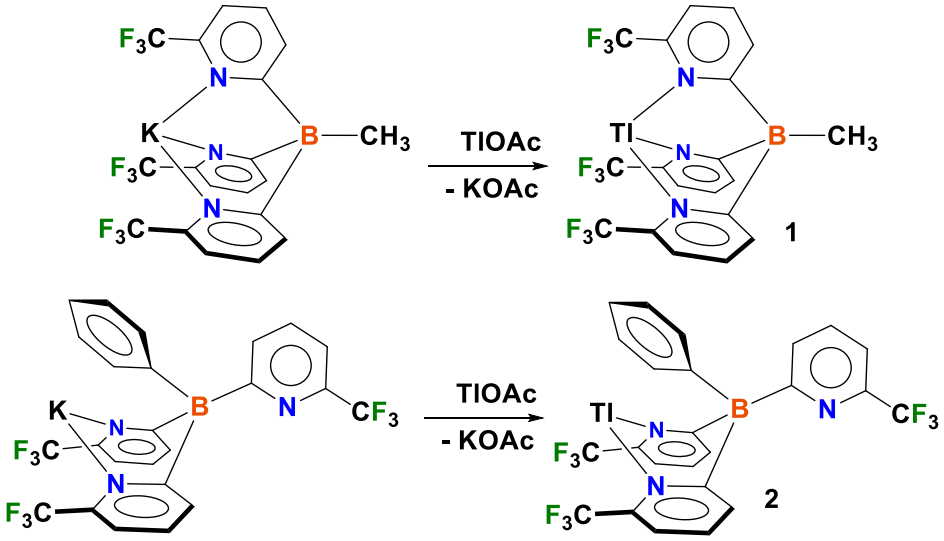

Scheme 1. Synthesis of [MeB(6-(CF_3)Py)$_3$]Tl (**1**) and [PhB(6-(CF_3)Py)$_3$]Tl (**2**) from their tris(pyridyl)borato potassium salts and TlOAc.

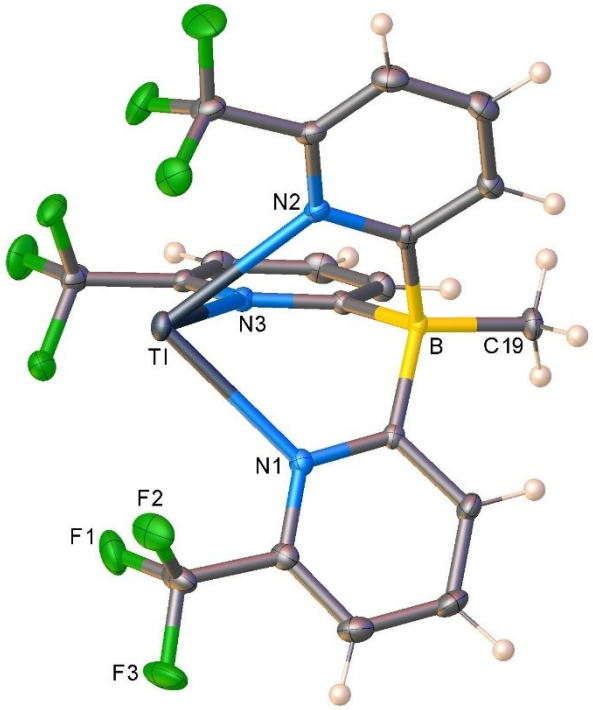

Figure 3. Molecular structure of [MeB(6-(CF_3)Py)$_3$]Tl (**1**) from single crystal X-ray diffraction.

Compounds **1**, **2** and **4** have been characterized in the solid-state by X-ray diffraction. The molecular structure of [MeB(6-(CF_3)Py)$_3$]Tl (**1**) is illustrated in Figure 3. Selected bond distances and angles are summarized in Table 1 (and given in supporting information). Thallium salt **1** features a κ^3-*NNN* bound tris(pyridyl)borate. The closest intermolecular Tl•••Tl separations at 6.35 Å exclude any significant interactions between thallium atoms in the solid state, and can be compared to the 3.6468(4) Å Tl-Tl distance of tetrameric {[HB(3-(cyclopropyl)Pz)$_3$]Tl}$_4$ or the sum of Bondi's van der Waals contact distance of 3.92 Å for two thallium atoms.[16, 35] Although there are no tris(pyridyl)boratothallium adducts available for a comparison, structural data of the closely related pyrazolyl analog **3** is available for a meaningful evaluation of the two classes of scorpionates.[2-3] The trigonal pyramidal coordination environment around thallium observed in **1** is similar to those reported for κ^3-*NNN* bound thallium(I) tris(pyrazolyl)borates including **3**.[9-10, 36] The Tl-N distances (Table 1) of **1** and **3** are similar despite having two different types of N-based heterocyclic donor arms in the two systems. All these Tl-N distances are however, longer than the sum of the covalent radii of Tl and N (2.16 Å),[37] but significantly shorter than

Bondi's van der Waals contact radius of Tl and N (3.51 Å).[35] The Tl•••C (of CF_3) separations (Table 1) and C-F•••Tl separations are notably shorter in the tris(pyridyl)borato complex **1**. Furthermore, space filling representations given in Figure 4 provide a visual representation of the different steric impacts of the two fluorinated ligand systems on thallium. The thallium center is more exposed in **3**. Yet another and more quantitative approach concerns buried volume ($\%V_{bur}$) calculations and steric maps, in which the $\%V_{bur}$ corresponds to the fraction of the volume of a sphere centered on the metal occupied by the coordinated ligand of focus, while the topographic steric map provides a graphical representation of the steric profile of a ligand using color-coded contour maps.[38-39] They indicate that $[MeB(6\text{-}(CF_3)Py)_3]^-$ is significantly more sterically demanding than that of $[MeB(3\text{-}(CF_3)Pz)_3]^-$ (Figure 5). For example, the $\%V_{bur}$ for **1** and **3** are 63.0 and 51.9, respectively. The former 63.0% approaches the regime of rather bulky tris(pyrazolyl)borates, e.g., $\%V_{bur}$ of tris(pyrazolyl)borates in $[HB(3\text{-}(Adamantyl)\text{-}5\text{-}(i\text{-}Pr)Pz)_3]Tl$[40] and $[HB(3\text{-}(t\text{-}Bu)\text{-}5\text{-}(i\text{-}Pr)Pz)_3]Tl$[41] are 64.6% and 59.4%, respectively.

Table 1. Selected bond distances, and angles of [MeB(6-(CF_3)Py)$_3$]Tl (**1**), [MeB(3-(CF_3)Pz)$_3$]Tl (**3**), [PhB(6-(CF_3)Py)$_3$]Tl (**2**), and [PhB(3-(CF_3)Pz)$_3$]Tl (**4**). The M•••C(B) is the *ipso*-carbon separation between the Tl and flanking phenyl group.

	[MeB(6-(CF_3)Py)$_3$]Tl (**1**)	[MeB(3-(CF_3)Pz)$_3$]Tl (**3**)	[PhB(6-(CF_3)Py)$_3$]Tl (**2**)[a]	[PhB(3-(CF_3)Pz)$_3$]Tl (**4**)
Tl-N (Å)	2.650(2) 2.639(2) 2.635(2)	2.601(2) 2.6228(15) 2.6228(15)	2.716(3), 2.698(3); *2.673(3),* *2.701(3)*	2.766(3) 2.739(3)
N-Tl-N (°)	81.96(6) 73.22(6) 73.41(6)	73.38(7) 70.17(5) 70.17(5)	71.53(10); *69.31(10)*	67.74(8)
Tl•••B (Å)	3.68	3.81	3.49; *3.46*	3.58
Tl•••C(B) (Å)	-	-	2.836(4); *2.844(4)*	3.001(3)
Tl•••Ph(centroid) (Å)	-	-	3.04; *3.04*	3.13
Average Tl•••C (of CF_3) (Å)	3.45	3.79	3.57; *3.56*	4.07
%V_{bur}	63.0	51.9	av. 58.8	47.4
Ref	This work	[30]	This work	This work

[a]Values for two crystallographically independent molecules, of which metrical parameters of the second molecule of [PhB(6-(CF_3)Py)$_3$]Tl are given in italics

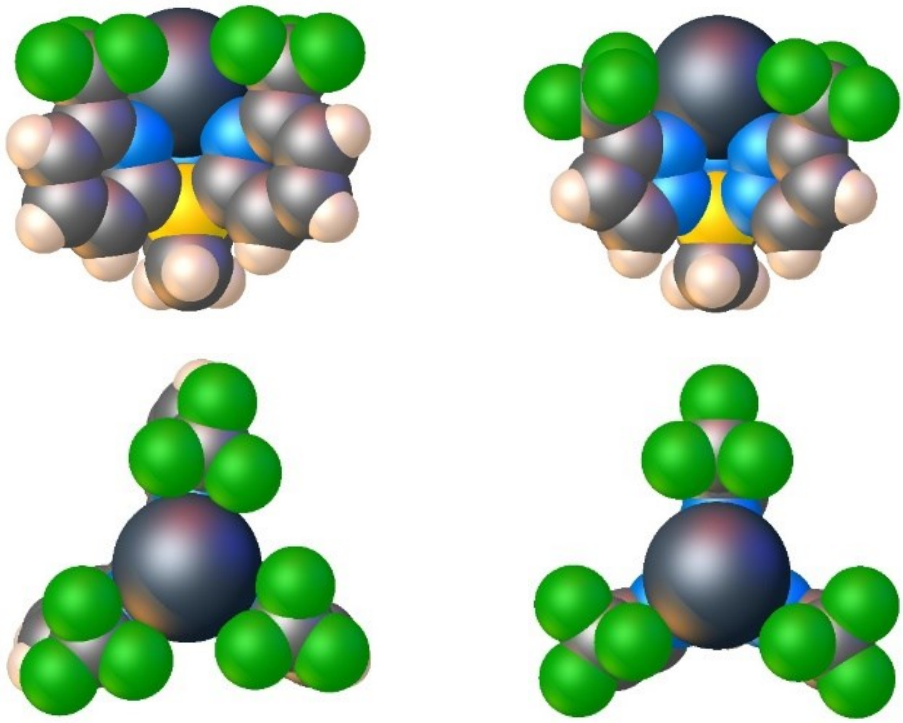

[MeB(6-(CF$_3$)Py)$_3$]Tl [MeB(3-(CF$_3$)Pz)$_3$]Tl

Figure 4. Orthogonal views of the space filling representation of [MeB(6-(CF$_3$)Py)$_3$]Tl (**1**) and [MeB(3-(CF$_3$)Pz)$_3$]Tl (**3**).

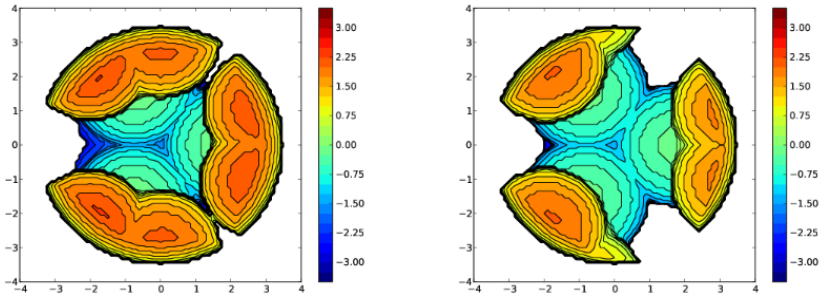

[MeB(6-(CF$_3$)Py)$_3$]Tl [MeB(3-(CF$_3$)Pz)$_3$]Tl

Figure 5. Steric maps for tris(pyridyl)borate and tris(pyrazolyl)borate ligands in [MeB(6-(CF$_3$)Py)$_3$]Tl (**1**) and [MeB(3-(CF$_3$)Pz)$_3$]Tl (**3**), looking down the Tl•••B axis.

The ^{19}F NMR spectrum of **1** in $CDCl_3$ displays a doublet[42-43] centered at δ -64.47 ppm, with $^4J_{Tl\text{-}F}$ of 1208 Hz. The related fluorine signal of the CF_3 groups of **3** under similar conditions ($CDCl_3$ at room temperature) appears as a doublet centered at δ –59.1, but with a substantially smaller $^4J_{Tl\text{-}F}$ = 880 Hz. In fact, $^4J_{Tl\text{-}F}$ is one of the largest values observed (other molecules with larger Tl-F spin-spin coupling have been reported such as $[CpMo(SC_6F_5)_2(CO)_2Tl]$ and $[CpMo(SC_6F_5)_4Tl]$ with $^4J_{Tl\text{-}F}$ of 3770 Hz at -100 °C and 3630 Hz at -100 °C, respectively, for some of the fluorine substituents),[44-45] and the largest to our knowledge among thallium scorpionates (see Table S1). The closer through-space approach of CF_3 fluorines of **1** compared to those of **3** could explain this larger Tl-F spin-spin coupling observed in the former (see Figure 4 and Table 1). These values also suggest that the thallium atoms remain in the coordination cavity of the scorpionate ligand in $CDCl_3$ solutions at room temperature.

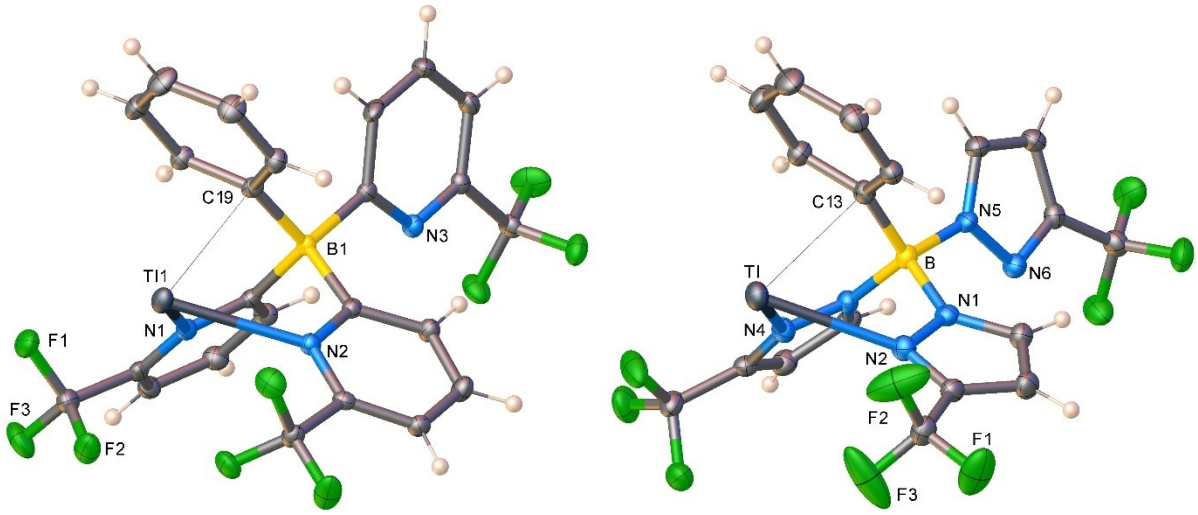

Figure 6. Molecular structure of $[PhB(6\text{-}(CF_3)Py)_3]Tl$ (**2**) (left) and $[PhB(3\text{-}(CF_3)Pz)_3]Tl$ (**4**) (right) from single crystal X-ray diffraction.

The B-phenyl substituted tris(pyridyl)borate complex $[PhB(6\text{-}(CF_3)Py)_3]Tl$ (**2**) crystallizes in $P2_1/n$ with two chemically similar but crystallographically different molecules in the asymmetric unit. Both $[PhB(6\text{-}(CF_3)Py)_3]Tl$ (**2**) and $[PhB(3\text{-}(CF_3)Pz)_3]Tl$ (**4**) display similar κ^2-*N,N* coordination modes

to thallium while the phenyl groups, rather than the third pyridyl or pyrazolyl arm occupy the space above the N-Tl-N plane (Figure 6). The Tl-N distances of κ^2-*N,N* bound **2** and **4** are longer than the corresponding distances observed for κ^3-*N,N,N* bound **1** and **3**, respectively, perhaps indicating the presence of significant arene-Tl interactions (Table 1). The boat shaped, 6-membered $Tl(NC)_2B$ core of **2** is deeper than the $Tl(NN)_2B$ core of **4** as evident from closer Tl•••B separations of the former. The borate phenyl groups of **2** and **4** are oriented above thallium and interact with these metal center in a π-fashion, with five ring carbon atoms (and with closest Tl •••C separation of 2.84 and 3.00 Å, respectively) residing within the Bondi's Tl-C van der Waals contact distance of 3.66 Å.[46] For comparison, the sum of the covalent radii of Tl and C_{sp2} is 2.18 Å.[37] Furthermore, the observed thallium-centroid separations of 3.04 and 3.13 Å, respectively for **2** and **4** are within the typical thallium•••centroid distances (2.85-3.18 Å)[47] observed for other structurally characterized Tl-π-arene complexes,[47-49] and similar to that noted for the mono(pyrazolyl)borate complex, $[Ph(Pz)BC_5H_{10}]Tl$ with a thallium•••centroid distance of 2.959 Å.[50] The closest intermolecular Tl•••Tl separations of **2** and **4** at 5.83 and 6.38 Å, respectively exclude any noteworthy interactions between thallium atoms in the solid state. The $[PhB(3\text{-}(CF_3)Pz)_3]Tl$ (**4**) crystal structure shows intermolecular π-interactions between the thallium atom and two pyrazolyl ring carbons of the adjacent molecule (closest at 3.44 and 3.47 Å) and nitrogen atom of the third pyrazolyl arm (at 3.27 Å) giving infinite *zig-zag* chains, see Figure S30. This could be the cause for slightly longer Tl-N distances of **4** compared to the corresponding bond lengths of **2** (Table 1). These intermolecular interactions of **4** are similar to those reported for $[(3,4,5\text{-}(F)_3C_6H_2)B(Pz)_3]Tl$ but the latter features a bridging asymmetric κ^3-*N,N,N* tris(pyrazolyl)borate coordination mode with much shorter intermolecular Tl-N bonds at 2.741 Å.[11]

The molecular structure of $[PhB(3\text{-}(CF_3)Pz)_3]Tl$ (**4**) may be contrasted with that of the [PhB(3-(*t*-Bu)Pz)$_3$]Tl reported by Parkin *et al*.[51] Although they both have tris(pyrazolyl)borate ligands with two pyrazolyl arms σ-bonded to the thallium sites (with Tl-N distances of 2.766(3) and 2.739(3) Å in **4** and

significantly shorter 2.585(3) and 2.528(3) Å for the latter), the third pyrazolyl group of [PhB(3-(*t*-Bu)Pz)$_3$]Tl, despite having a larger *t*-butyl substituent on the ring (relative to CF_3 substituents of **4**), positions above the thallium center but rotated about 90° allowing a close interaction between thallium and the nitrogen attached directly to the boron via a p-orbital component of the aromatic π-system (at Tl-N separation of 2.833(2) Å). The B-phenyl group of [PhB(3-(*t*-Bu)Pz)$_3$]Tl occupies the axial site of the six-membered chair-shaped B(N_2N_2)Tl core. However, both isomers are present in solution (as evident from NMR data at -80 °C) in which pyrazolyl moieties either occupying the axial sites of the B(N_2N_2)Tl core as in **4** or equatorial sies as observed in the solid state structure of [PhB(3-(*t*-Bu)Pz)$_3$]Tl. At room temperature, [PhB(3-(*t*-Bu)Pz)$_3$]Tl is stereochemically non-rigid on the NMR spectroscopic time scale (just like **4** as noted below), pointing to only a small energy difference between the two isomers.

Space filling representations given in Figure 7 provide a visual representation of the different steric impacts of the two B-phenylated and fluorinated ligand systems on thallium in **2** and **4**. As evident from these views, tris(pyridyl)borate provides a greater protection to thallium. Steric demands of the two ligands of thallium have also been quantified using the buried volume concept, which indicate that the scorpionate in **2** and **4** has $\%V_{bur}$ of 58.8 (average for two crystallographically independent molecules in the asymmetric unit) and 47.4, respectively. These values for B-phenylated scorpionates on thallium are smaller than the corresponding B-methylated systems for each ligand class, which is not surprising as the latter features more "closed" κ^3-*NNN* bound ligands.

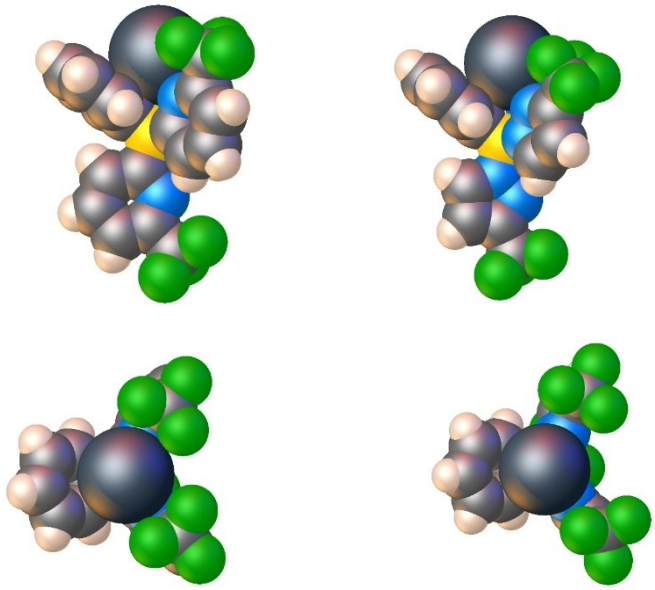

[PhB(6-(CF$_3$)Py)$_3$]Tl [PhB(3-(CF$_3$)Pz)$_3$]Tl

Figure 7. Orthogonal views of the space filling representation of [PhB(6-(CF$_3$)Py)$_3$]Tl (**2**) and [PhB(3-(CF$_3$)Pz)$_3$]Tl (**4**).

The ^{19}F NMR spectrum of **2** in CDCl$_3$ displays an overlapping broad doublet and a singlet corresponding to CF$_3$ fluorine resonances of the thallium bound and free pyridyl moieties. Broad signals suggest that the molecule is stereochemically nonrigid in chloroform on the NMR spectroscopic time scale at room temperature with coordinated and free pyridyl arms exchanging slowly, perhaps via the involvement of $\kappa^2 \leftrightarrow \kappa^3 \leftrightarrow \kappa^2$ coordination modes. Cooling to -10 °C slows down this dynamic process sufficiently to observe different, yet very broad ^{19}F NMR signals for the two pyridyl groups but they sharpen around -50 °C producing a clear doublet with $^4J_{\text{Tl-F}}$ of 1100 Hz for the thallium(I) bound arms and a singlet for the remote pyridyl moiety (Figure S19). The coupling constant value does not change much from -20 to -50 °C. It is also one of the notably high $^4J_{\text{Tl-F}}$ values observed in thallium chemistry

(Table S1), and closer to that of **1**. The B-phenylated tris(pyrazolyl)borate thallium complex **4** in $CDCl_3$ exhibits a broad doublet (or a sharp singlet in DMSO-d_6) at room temperature for the CF_3 groups (Figure S21). Data suggest the presence of three equivalent pyrazolyl arms on the NMR time scale, and a highly fluxional system and faster interconversion of bound and free pyrazolyl moieties under these conditions. Interestingly, both **2** and **4** crystallize with the "donor" nitrogen atom of the free pyridyl and pyrazolyl ligand arms with an easy swing at the metal site (Figure 6) between the wedge created by the two bound arms. If these pre-aligned conformations were to retain in solution, they would facilitate an easy backside attack on thallium and $\kappa^2 \leftrightarrow \kappa^3 \leftrightarrow \kappa^2$ interconversion.

In order to evaluate differences between κ^2- and κ^3-coordination modes, and their plausible interconversion indicated from NMR, we performed density functional calculations (DFT) for the molecules of focus in this work and several other related species. For [MeB(6-(CF_3)Py)$_3$]Tl (**1**) and [MeB(3-(CF_3)Pz)$_3$]Tl (**3**), the κ^3-coordination is favored over the κ^2-mode by 5.8 and 8.9 kcal/mol (Table S11), respectively. In the pyridyl case **1**, a larger stabilization from electronic effects (i.e., orbital and electrostatic interactions) overshadows enhanced, yet relatively smaller repulsive Pauli term (owing to the steric crowding or steric effects) favoring the observed κ^3-coordination mode, while in the pyrazolyl counterpart **3** both stabilizing and destabilizing contributions are relatively smaller than those computed for **1**, but again somewhat favorable electronic effects stabilize the κ^3-isomer. Interestingly, the possible $\kappa^3 \leftrightarrow \kappa^2$ interconversion is enabled following a rotation of the MeB- fragment leading to the detachment of a pyridyl/pyrazolyl ring from the κ^3-mode and varying the orientation of two coordinating rings to achieve a κ^2-mode (Figure 8). Such transformation involves a transition state at 13.6 and 15.7 kcal/mol, above the favored κ^3-coordination mode observed in X-ray crystal structures.

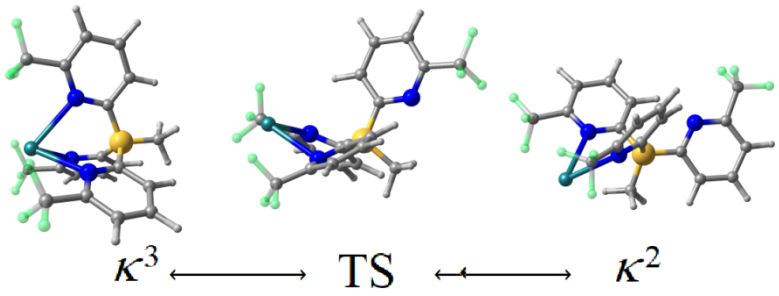

Figure 8. Evaluated structures and transition state (TS) related to the $\kappa^3 \leftrightarrow \kappa^2$ interconversion mechanism [MeB(6-(CF_3)Py)$_3$]Tl (**1**).

The κ^2-coordination mode with the phenyl ring flanking the Tl atom is favored in comparison to κ^3-isomer by 7.2 and 3.0 kcal/mol for the B-phenylated species [PhB(6-(CF_3)Py)$_3$]Tl (**2**) and [PhB(3-(CF_3)Pz)$_3$]Tl (**4**), respectively. For **2**, much favorable electronic effects dominate unfavorable steric effects leading to the observed κ^2-mode. Interestingly for **4**, κ^2-mode is sterically preferred, which overshadows the favorable orbital term in κ^3-mode coordination, resulting in the observed κ^2-mode albeit by a smaller margin. Overall, DFT predictions are in excellent agreement with the observed molecular structures of **1-4** in the solid-state.

In compounds **2** and **4**, the alternative orientation of the phenyl ring, occupying the equatorial sites of the boat shaped six-membered Tl(N_2C_2)B or Tl(N_2N_2)B cores, with the detached pyridyl/pyrazolyl ring above the Tl atom, is less favored by 6.3 and 2.5 kcal/mol respectively, against the observed structures (with flanking phenyl ring over thallium). In these systems, the $\kappa^3 \leftrightarrow \kappa^2$ interconversion involves a transition state of 19.3 and 12.8 kcal/mol above the favored κ^2-mode, accounting for the fluxional behavior observed in NMR experiments. The computed values show that the replacement of ring–CF_3 substituents by –CH_3 in **2** and **4** would result in molecules with κ^2-coordination mode but favored only by a smaller energy difference of 1.6 and 0.6 kcal/mol over the κ^3-mode, respectively, and likely leading to a more facile fluxional behavior solution. Moreover, the computed data for the molecule involving the

replacement of –CF_3 substituents of **2** by *t*-butyl groups show a preferred κ^2-mode (over κ^3-coordination) by 4.8 kcal/mol for the pyridyl case.

Calculations of the ring *t*-butyl substituted version of **4** predict an asymmetrical κ^3-coordination mode with a *t*-butyl pyrazolyl arm at an axial position over thallium, and N-Tl distances of 2.534, 2.617, and a Tl-N(B) of 2.919 Å. As noted earlier, observed structure of [PhB(3-(*t*-Bu)Pz)$_3$]Tl in the solid-state[51] also has all three pyrazolyl moieties on the thallium side, with one of those adopting a side-on coordination as predicted by DFT. This structure is favored over the κ^2-isomer with an axial phenyl group by 2.6 kcal/mol, while the isomer with symmetrical κ^3-coordination mode with the three N-Tl distances constrained to similar values (2.563, 2.685, and 2.714 Å) is less stable by 9.4 kcal/mol, in comparison to the κ^2-mode. Overall, the preferred coordination mode is determined by the balance between steric (destabilizing) and various electronic (stabilizing) factors present in different isomers.

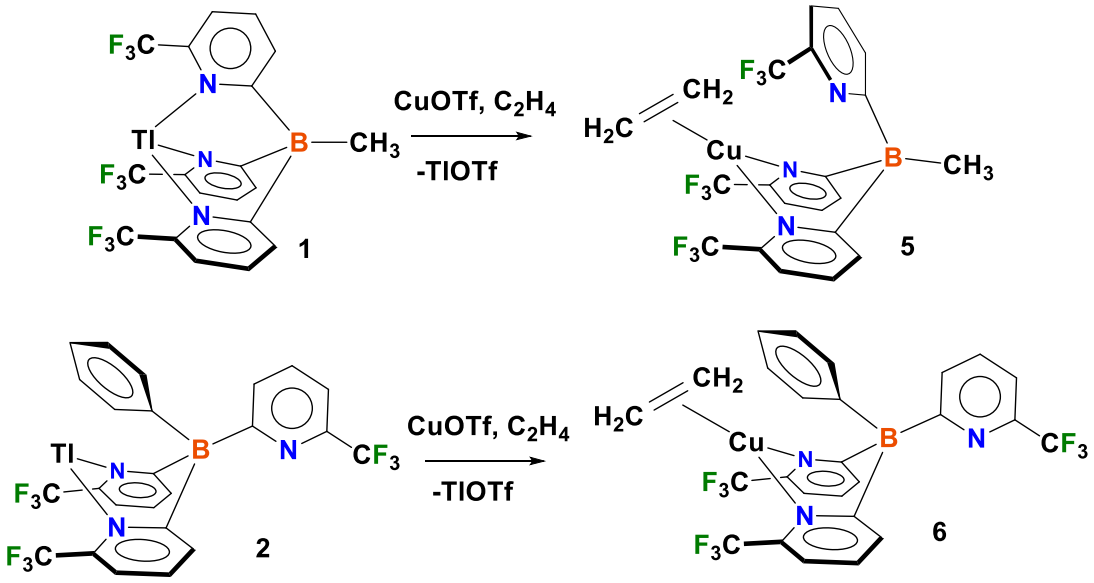

Scheme 2. Synthesis of [MeB(6-(CF_3)Py)$_3$]Cu(C_2H_4) (**5**) and [PhB(6-(CF_3)Py)$_3$]Cu(C_2H_4) (**6**) from their tris(pyridyl)borato thallium precursors, CuOTf and ethylene.

The ligand transfer prowess of tris(pyrazolyl)borate thallium compounds is well known.[2, 9-10] In fact, [MeB(3-(CF_3)Pz)$_3$]Tl (**3**) allows the synthesis of the copper(I) ethylene complex [MeB(3-(CF_3)Pz)$_3$]Cu(C_2H_4) very effectively.[30] Similarly, [MeB(6-(CF_3)Py)$_3$]Tl (**1**) undergoes metal ion exchange smoothly with copper(I) triflate in the presence of ethylene producing [MeB(6-(CF_3)Py)$_3$]Cu(C_2H_4) (Scheme 2, **5**),[23] which has been obtained previously using a route utilizing [MeB(6-(CF_3)Py)$_3$]K. The thallium complex of the B-Ph ligand version [PhB(6-(CF_3)Py)$_3$]Tl (**2**) also serves as a good scorpionate transfer agent. For example, it reacts with copper(I) triflate under an ethylene atmosphere to afford [PhB(6-(CF_3)Py)$_3$]Cu(C_2H_4) (**6**) in good yield (Scheme 2). The ^{1}H and ^{13}C NMR chemical shifts of the ethylene proton and carbon resonances of **6** were observed at δ 3.59 and 85.1, respectively. The ethylene proton resonance of this molecule appears at a notably upfield region relative to the free ethylene chemical shift (δ 5.40 ppm). This is diagnostic of the tris(pyridyl)borate in **6** serving as a κ^2-donor to copper with an aromatic ring system occupying the position above the Cu-ethylene moiety. Such an arrangement usually leads to an aromatic ring current effect on ethylene proton signals and to greater shielding[52] as observed before in [PhB(3-(C_2F_5)Pz)$_3$]Cu(C_2H_4),[53] and [(*t*-BuC_6H_4)B(6-(CF_3)Py)$_3$]Cu(C_2H_4)[21] that feature κ^2-bound scorpionates and flanking B-aryl groups, as well as in **5** (which has a flanking pyridyl moiety). The ^{19}F NMR spectrum of **6** (Figure S25) displays two clearly resolved signals for bound and free pyridyl moieties.

Summary

We describe the successful syntheses of thallium(I) complexes of tris(pyridyl)borates and a comparison to their tris(pyrazolyl)borate relatives. The B-methylated [MeB(6-(CF_3)Py)$_3$]Tl displays κ^3-coordination of the tris(pyridyl)borate similar to tris(pyrazolyl)borate in [MeB(3-(CF_3)Pz)$_3$]Tl, while [PhB(6-(CF_3)Py)$_3$]Tl and [PhB(3-(CF_3)Pz)$_3$]Tl feature κ^2-*NN* ligand coordination modes with the B-phenyl groups flanking the thallium sites. The X-ray structural and percent buried volume data indicate that these trifluoromethylated tris(pyridyl)borate ligands provide greater steric protection than their

tris(pyrazolyl)borate counterparts. The CF_3 groups are much closer through space to the thallium sites in the tris(pyridyl)borates. The ^{19}F NMR spectroscopy of [MeB(6-(CF_3)Py)$_3$]Tl reveals a remarkably large 1208 Hz four-bond thallium-fluorine coupling constant in chloroform at room temperature, which is considerably larger than that observed for the pyrazolyl borate analog. This is most likely a result of through-space coupling. The [PhB(6-(CF_3)Py)$_3$]Tl is fluxional at room temperature in chloroform, but the presumed intramolecular behavior involving alternate ligand-binding modes can be slowed to the NMR time scale by cooling to afford a four-bond thallium-fluorine coupling constant of 1110 Hz in the ^{19}F spectrum. The tris(pyridyl)borate complexes [MeB(6-(CF_3)Py)$_3$]Tl and [PhB(6-(CF_3)Py)$_3$]Tl are competent ligand transfer agents as demonstrated by their use in the synthesis of copper(I) ethylene complexes bearing the tris(pyridyl)borate ligand supports. We are currently examining thallium coordination and ligand transfer chemistry of various poly(pyridyl)borates including those of the bis(pyridyl)borates.

Experimental section

General information: All preparations and manipulations were carried out under an atmosphere of purified nitrogen using standard Schlenk techniques or in an MBraun drybox equipped with a -25 °C refrigerator. Chloroform was dried over CaH_2 and distilled. Dichloromethane and hexane were dried by passing HPLC grade solvent through a Solvent Purification System (SPS, innovative technologies inc.) and stored in Straus flasks. Tetrahydrofuran was distilled from a sodium/ketyl still. Glassware was oven dried overnight at 150 °C. NMR spectra were acquired at 25 °C (unless noted) on a JEOL Eclipse 500 spectrometer (^1H, 500 MHz; ^{13}C, 126 MHz; ^{19}F, 471 MHz), JEOL Eclipse 300 spectrometer (^1H, 300 MHz; ^{13}C, 76 MHz; ^{19}F, 273 MHz; ^{11}B, 96 MHz), JEOL Eclipse 400 spectrometer (^1H, 400 MHz; ^{19}F, 376 MHz) and all the spectral data were processed on MNova or JEOL Delta. ^{19}F NMR values were referenced to external $CFCl_3$. ^{11}B spectra were externally referenced to BF_3•Et_2O in $CDCl_3$ (δ = 0 ppm). ^1H and ^{13}C NMR spectra were referenced internally to solvent signals ($CDCl_3$: 7.26 ppm for ^1H NMR,

77.16 ppm for ^{13}C NMR; DMSO-d_6: 2.50 ppm for ^{1}H NMR, 39.52 ppm for ^{13}C NMR), or externally to $SiMe_4$ (0 ppm). ^{1}H, ^{13}C,^{19}F, and ^{11}B NMR chemical shifts are reported in ppm and coupling constants (J) are reported in Hertz (Hz). Abbreviations used for signal assignments: Py = pyridyl, Py^n = noncoordinated pyridyl, Ph = Phenyl, Me = Methyl, s = singlet, d = doublet, dd = doublet of doublets, t = triplet, q = quartet, m = multiplet, brs = broad singlet. NMR solvents were purchased from Cambridge Isotopes Laboratories and used as received. Ethylene gas was purchased from Matheson. Elemental analyses were performed using a Perkin-Elmer Model 2400 CHN analyzer. High-resolution (HR) mass spectra were recorded at Shimadzu Center Laboratory for Biological Mass Spectrometry at UTA. The compounds {(6-(CF_3)-2-Py)MgCl}$_2$•$(THF)_x$[23] and $PhBBr_2$[54] were prepared by modified literature procedures. The $[Cu(OTf)]_2$•C_7H_8[55] as prepared according to literature procedures. All other reagents were obtained from commercial sources and used as received.

Note: Thallium salts are poisonous; accordingly, these compounds should be handled with the appropriate precautions and waste products must be disposed of properly.

Synthesis of [MeB(6-(CF_3)Py)$_3$]Tl (1).

To a mixture of [MeB(6-(CF_3)Py)$_3$]K (300 mg, 596 μmol) and TlOAc (236 mg, 894 μmol) in a 50 mL Schlenk flask, 25 mL of anhydrous chloroform was added, and the mixture was then refluxed for 4 hours. After cooling to room temperature, the reaction mixture was cannula-filtered through a celite-packed frit to remove KOAc and excess TlOAc. The solvent was then removed under reduced pressure, resulting in a pale, yellow-colored solid. Single crystals of [MeB(6-(CF_3)Py)$_3$]Tl, suitable for X-ray analysis, were grown by slow evaporation of its chloroform solution at room temperature. Yield: 310 mg (78%). ^{1}H NMR (500 MHz, $CDCl_3$): δ (ppm) 7.97 (d, J = 7.7 Hz, 3H, Py), 7.64 (t, J = 7.8 Hz, 3H, Py), 7.43 (d, J = 7.7 Hz, 3H, Py), 0.77 (s, 3H, BMe). $^{13}C\{^{1}H\}$ NMR (126 MHz, $CDCl_3$): δ (ppm) 186.7 (q, $^{1}J_{C–B}$ = 52.8 Hz, Py), 145.2 (q, $^{2}J_{C–F}$ = 32.4 Hz, Py), 135.7 (Py), 132.6 (Py), 122.9 (q, $^{1}J_{C–F}$ = 275.9 Hz, CF_3), 117.2 (Py), 12.6 (q, $^{1}J_{C–B}$ = 46.8 Hz, BMe). ^{19}F NMR (471 MHz, $CDCl_3$): δ (ppm) -64.47 (d, $^{4}J_{Tl-F}$ = 1208 Hz).

^{11}B NMR (96 MHz, $CDCl_3$): δ (ppm) -11.54. HR-MS [ESI, positive ion mode ESI-TOF]: m/z for $C_{19}H_{13}B_1F_9N_3Tl_1$ $[M+H]^+$ calcd: 670.0803. Found: 670.0844. **Crystal Data** for $C_{19}H_{12}BF_9N_3Tl$ (M =668.50 g/mol): triclinic, space group P-1 (no. 2), a = 8.1808(6) Å, b = 9.3866(7) Å, c = 14.3023(11) Å, α = 75.7770(10)°, β = 76.1460(10)°, γ = 71.0390(10)°, V = 991.46(13) Å^3, Z = 2, T = 99.99 K, μ(Mo Kα) = 8.241 mm^{-1}, *Dcalc* = 2.239 g/cm^3, 11560 reflections measured (4.668° ≤ 2Θ ≤ 61°), 5707 unique (R_{int} = 0.0242, R_{sigma} = 0.0335) which were used in all calculations. The final R_1 was 0.0201 (I > 2σ(I)) and wR_2 was 0.0489 (all data).

Synthesis of [PhB(6-(CF$_3$)Py)$_3$]H. A solution of dibromo(phenyl)borane (6.0 g, 24.22 mmol) in anhydrous toluene (50 mL) at 0 °C was added to a suspension of {(6-(CF$_3$)-2-Py)MgCl}$_2$•(THF)$_3$ (30.40 g, 48.44 mmol) in anhydrous toluene (200 mL) at 0 °C. After stirring at 0 °C for 2 hours, the reaction mixture was slowly warmed to room temperature and stirred for an additional 24 hours. The resulting mixture was poured into water (250 mL) and ethyl acetate (200 mL) mixture with the addition of 5 g of Na_2CO_3. After stirring for 2 hours, the layers were separated, and the aqueous layer was extracted with ethyl acetate (3 × 25 mL). The organic extracts were combined, washed with brine, dried over Na_2SO_4, and evaporated to dryness. The residue was purified through silica gel column chromatography using hexane and ethyl acetate (9:1) as the eluent, yielding the desired [PhB(6-(CF$_3$)Py)$_3$]H as a white solid. Yield: 8.6 g (67%). ^{1}H NMR (500 MHz, $CDCl_3$): δ (ppm) 18.99 (brs, NH), 7.76 – 7.69 (m, 6H, Py), 7.52 (dd, J = 7.3, 1.4 Hz, 3H, Py), 7.23 – 7.15 (m, 5H, Ph). ^{13}C{^{1}H} NMR (126 MHz, $CDCl_3$): δ (ppm) 184.5 (q, $^1J_{C–B}$ = 54.0 Hz, Py), 154.0 (q, $^1J_{C–B}$ = 46.8 Hz, Ph), 142.7 (q, $^2J_{C–F}$ = 36.0 Hz, Py), 136.6 (Ph/Py), 134.9 (Ph/Py), 134.6 (Ph/Py), 127.7 (Ph/Py), 125.4 (Ph/Py), 121.5 (q, $^1J_{C–F}$ = 274.7 Hz, CF_3), 117.2 (Ph/Py). ^{19}F NMR (471 MHz, $CDCl_3$): δ (ppm) -67.81 (s). ^{11}B NMR (96 MHz, $CDCl_3$): δ (ppm) -10.79. Anal. Calc. $C_{24}H_{15}B_1F_9N_3$: C, 54.68%; H, 2.87%; N, 7.97%. Found: C, 54.33%; H, 2.84%; N, 7.76%. HR-MS [ESI, positive ion mode ESI-TOF]: m/z for $C_{24}H_{16}B_1F_9N_3$ $[M+H]^+$ calcd: 528.1293. Found: 528.1295

Synthesis of [PhB(6-(CF$_3$)Py)$_3$]K

To a suspension of KH (0.100 g, 2.49 mmol) in 20 mL of THF at 0 °C, a solution of [PhB(6-(CF$_3$)Py)$_3$]H (1.20 g, 2.28 mmol) in 20 mL of THF was slowly added via cannula transfer. After the complete cessation of hydrogen gas evolution, the reaction was allowed to warm to room temperature and was stirred overnight. The resulting yellow solution was filtered through a celite-packed frit to remove any unreacted KH. The colorless filtrate was concentrated under reduced pressure to obtain [PhB(6-(CF$_3$)Py)$_3$]K as an off-white solid. The compound was further dried at 60 °C under reduced pressure overnight to remove any trace solvent. Yield: 1.23 g (95%). ^{1}H NMR (300 MHz, DMSO-d$_6$): δ 7.61 (d, *J* = 7.6 Hz, 3H, Py), 7.50 (t, *J* = 7.7 Hz, 3H, Py), 7.30 (d, *J* = 7.4 Hz, 3H, Py), 7.22 (brs, 2H, Ph), 6.97 (t, *J* = 7.2 Hz, 2H, Ph), 6.87 (t, *J* = 6.9 Hz, 1H, Ph).^{13}C{^{1}H} NMR (76 MHz, DMSO-d$_6$): δ (ppm) 188.0 (q, $^1J_{C\text{-}B}$ = 56.3 Hz, Py), 159.7 (q, $^1J_{C\text{-}B}$ = 50.0, Ph), 144.5 (q, $^2J_{C\text{-}F}$ = 31.8 Hz, Py), 135.1 (Py/Ph), 132.8 (Py/Ph), 132.6 (Py/Ph), 125.8 (Py/Ph), 122.9 (q, $^1J_{C\text{-}F}$ = 273.8 Hz, CF3), 122.6 (Py/Ph), 114.2 (Py/Ph).^{19}F NMR (273 MHz, DMSO- d$_6$): δ (ppm) -66.25. ^{11}B NMR (96 MHz, DMSO- d$_6$): δ (ppm) -7.02. Anal. Calc. C$_{24}$H$_{14}$B$_1$F$_9$N$_3$K$_1$: C, 50.99%; H, 2.50%; N, 7.43%. Found: C, 50.65%; H, 2.18%; N, 7.15%. HR-MS [ESI, positive ion mode ESI-TOF]: m/z for C$_{24}$H$_{15}$B$_1$F$_9$N$_3$K$_1$ [M+H]$^+$ calcd: 566.0852. Found: 566.0867

Synthesis of [PhB(6-(CF$_3$)Py)$_3$]Tl (2).

[PhB(6-(CF$_3$)Py)$_3$]Tl was synthesized using an identical procedure to that of [MeB(6-(CF$_3$)Py)$_3$]Tl. The synthesis involved the use of [PhB(6-(CF$_3$)Py)$_3$]K (200 mg, 354 μmol) and TlOAc (140 mg, 531 μmol) as the reactants. The resulting product was obtained in the form of a white solid, which was subsequently washed with cold hexane to purify it. Single crystals of [PhB(6-(CF$_3$)Py)$_3$]Tl suitable for X-ray analysis were grown by slow evaporation of its chloroform solution at room temperature. Yield: 195 mg (75%). ^{1}H NMR (500 MHz, CDCl$_3$): δ (ppm) 7.87 (brs, 1H, Py/Ph), 7.58 (t, *J* = 7.8 Hz, 3H, Py/Ph), 7.44 –7.41

(m, 5H, Py/Ph), 7.32 (t, J = 7.3 Hz, 1H, Py/Ph), 7.13 (s, 2H, Py/Ph). ^{1}H NMR (400 MHz, $CDCl_3$ at -50 °C): δ (ppm) 8.09 (d, J = 7.5 Hz, 2H, Py/Ph), 7.64 – 7.55 (m, 3H, Py/Ph), 7.49 – 7.41 (m, 5H, Py/Ph), 7.34 (t, J = 7.1 Hz, 1H, Py/Ph), 7.04 – 6.97 (m, 3H, Py/Ph). $^{13}C\{^{1}H\}$ NMR (126 MHz, $CDCl_3$): δ (ppm) 184.4 (q, $^{1}J_{C-B}$ = 54.0 Hz, Py), 161.8 (br, Ph), 145.7 (q, $^{2}J_{C-F}$ = 33.6 Hz, Py), 137.7 (d, J = 59.4 Hz), 130.2 (d, J = 50.4 Hz), 135.2 (Py/Ph), 133.9 (Py/Ph), 130.2 (d, J = 50.4 Hz), 127.4 (Py/Ph), 123.0 (q, $^{1}J_{C-F}$ = 274.7 Hz, CF_3), 116.5 (Py/Ph). ^{19}F NMR (471 MHz, $CDCl_3$): overlapping doublet with the singlet δ (ppm) -65.57 (br d, coupling constant value cannot be computed reliably due to peak overlap), -66.57 (br s). ^{19}F NMR (376 MHz, $CDCl_3$ at -50 °C): δ (ppm) -64.52 (d, $^{4}J_{Tl-F}$ = 1110 Hz), -67.55 (s). ^{11}B NMR (96 MHz, $CDCl_3$): δ (ppm) -7.66. HR-MS [ESI, positive ion mode ESI-TOF]: m/z for $C_{24}H_{15}B_1F_9N_3Tl_1$ $[M+H]^+$ calcd: 732.0959. Found: 732.0932. **Crystal Data** for $C_{24}H_{14}BF_9N_3Tl$ (M =730.56 g/mol): monoclinic, space group $P2_1/n$ (no. 14), a = 10.5774(13) Å, b = 23.681(3) Å, c = 19.481(3) Å, β = 104.901(2)°, V = 4715.6(10) Å^3, Z = 8, T = 100.00 K, μ(Mo Kα) = 6.941 mm^{-1}, $Dcalc$ = 2.058 g/cm^3, 50852 reflections measured (1.72° ≤ 2Θ ≤ 57.398°), 12206 unique (R_{int} = 0.0254, R_{sigma} = 0.0223) which were used in all calculations. The final R_1 was 0.0268 (I > 2σ(I)) and wR_2 was 0.0658 (all data).

Synthesis of [PhB(3-(CF$_3$)Pz)$_3$]Tl (4): [PhB(3-(CF$_3$)Pz)$_3$]Li (0.26 g, 0.520 mmol) and thallium acetate (0.17 g, 0.626mmol) were mixed in a Schlenk tube filled with 30mL of THF at room temperature. This mixture stirred for about 5 hours, then filtered and the solvent was removed from the filtrate under reduced pressure to obtain the product as an off-white powder with a yield of 70%. It was recrystallized from hexanes to obtain colorless crystal of [PhB(3-(CF$_3$)Pz)$_3$]Tl. Mp.: 209 ºC. ^{1}H NMR (500 MHz, $CDCl_3$): δ (ppm) 7.55 (s, 3H, 5-*H*), 7.48-7.46 (m, 3H, Ph-*H*), 6.94 (d, J = 4.6 Hz, 2H, Ph-*H*), 6.52 (d, J = 1.6 Hz, 3H, 4-*H*). ^{19}F NMR (376 MHz, $CDCl_3$): δ (ppm) -60.71 (br d, $^{4}J_{Tl-F}$ = 388 Hz, CF_3). ^{11}B NMR (96 MHz, $CDCl_3$): δ (ppm) 1.20 (br s). Anal. Calc. for $C_{18}H_{11}BF_9N_6Tl$: C, 30.86; H, 2.01; N, 12.00%. Found: 31.43; H, 1.79; N, 11.68. **Crystal Data** for $C_{18}H_{11}BF_9N_6Tl$ (M = 697.51 g/mol): monoclinic, space group $P2_1/c$ (no. 14), a = 10.8269(4) Å, b = 16.6812(7) Å, c = 12.7052(5) Å, β = 108.5630(10)°, V = 2175.25(15) Å^3,

$Z = 4$, $T = 100.15$ K, μ(MoKα) = 7.521 mm^{-1}, *Dcalc* = 2.130 g/cm^3, 17935 reflections measured (3.968° ≤ 2Θ ≤ 53.462°), 4612 unique (R_{int} = 0.0573, R_{sigma} = 0.0465) which were used in all calculations. The final R_1 was 0.0272 (I > 2σ(I)) and wR_2 was 0.0722 (all data).

Synthesis of [MeB(6-(CF$_3$)Py)$_3$]Cu(C$_2$H$_4$) (5):

To a mixture of [MeB(6-(CF$_3$)Py)$_3$]Tl (100 mg, 150 μmol) and [Cu(OTf)]$_2$•C$_7$H$_8$ (39 mg, 75 μmol) was added anhydrous dichloromethane and then ethylene (1 atm) was bubbled into the solution. The reaction mixture was kept stirring for 3 hours, and then cannula filtered through Celite packed frit to remove TlOTf. The solvent was then removed under reduced pressure to obtain product as a white powder (75 mg, 90 %). The ^{1}H and ^{19}F spectral data were found to be consistent with the data reported previously.[30]

Synthesis of [PhB(6-(CF$_3$)Py)$_3$]Cu(C$_2$H$_4$) (6): To a mixture of [PhB(6-(CF$_3$)Py)$_3$]Tl (100 mg, 137 μmol) and [Cu(OTf)]$_2$•C$_7$H$_8$ (39 mg, 75 μmol) was added anhydrous dichloromethane and then ethylene (1 atm) was bubbled into the solution. The reaction mixture was kept stirring for 3 hours, and then cannula filtered through Celite packed frit to remove TlOTf. The solvent was then removed under reduced pressure to obtain product as a white powder. Yield: 78 mg (92 %). ^{1}H NMR (500 MHz, $CDCl_3$): δ (ppm) 7.85 (d, J = 7.5 Hz, 2H, Py), 7.68 (t, J = 7.8 Hz, 2H, Py), 7.56 (t, J = 7.8 Hz, 1H, Py^n), 7.51 (dd, J = 8.0, 1.3 Hz, 2H, Py), 7.47 (d, J = 7.7, 0.9 Hz, 1H, Py^n), 7.21-7.17 (overlapping, 3H, Ph), 6.88 (d, J = 7.5 Hz, 1H, Py^n), 6.85 (brs, 2H, Ph), 3.59 (s, 4H, C_2H_4).^{13}C{^{1}H} NMR (126 MHz, $CDCl_3$): δ (ppm) 185.6 (q, $^1J_{C–B}$ = 52.9 Hz, Py), 182.0 (q, $^1J_{C–B}$ = 59.0 Hz, Py^n), 154.2 (q, $^1J_{C–B}$ = 49.3 Hz, Ph), 146.8 (q, $^2J_{C–F}$ = 37.2 Hz, Py^n), 145.8 (q, $^2J_{C–F}$ = 37.3 Hz, Py), 137.5 (Ph), 136.1 (Py), 135.3 (Py^n), 134.1 (Py), 133.5 (Py^n), 127.8 (Ph), 126.5 (Ph), 122.7 (q, $^1J_{C–F}$ = 275.18 Hz, CF_3-Py^n), 121.9 (q, $^1J_{C–F}$ = 273.3 Hz, CF_3-Py), 118.1 (Py), 116.0 (Py^n), 85.1 (C_2H_4). ^{19}F NMR (471 MHz, $CDCl_3$): δ (ppm) -65.57 (s, 6F, CF_3−Py), -67.88 (s, 3F, CF_3−Py^n). ^{11}B NMR (96 MHz, $CDCl_3$): δ (ppm) -7.63. HR-MS [ESI, positive ion mode ESI-TOF]: m/z for $C_{24}H_{15}B_1F_9N_3Cu_1$ [M-C_2H_4+H]$^+$ calcd: 590.0511. Found: 590.0514.

X-ray Data Collection and Structure Determinations

A suitable crystal covered with a layer of hydrocarbon/Paratone-N oil was selected and mounted on a Cryo-loop, and immediately placed in the low temperature nitrogen stream. The X-ray intensity data were measured at 100 K (unless otherwise noted), on a SMART APEX II CCD area detector system equipped with an Oxford Cryosystems 700 series cooler, a graphite monochromator, and a Mo Kα fine-focus sealed tube (λ = 0.71073 Å). Intensity data were processed using the Bruker Apex program suite. Absorption corrections were applied by using SADABS.[56] Initial atomic positions were located by SHELXT,[57] and the structures of the compounds were refined by the least-squares method using SHELXL[58] within Olex2 GUI.[59] All the non-hydrogen atoms were refined anisotropically. Hydrogen atoms were included at calculated positions and refined using appropriate riding models. X-ray structural figures were generated using Olex2. Crystallographic data have been deposited with the Cambridge Crystallographic Data Centre (CCDC 2287574-2287576). Additional details are provided in supporting information section.

Supporting Information Available: Spectroscopic details, X-ray crystallographic data (CIF), computational details, and additional figures. This material is available free of charge via the Internet at http://pubs.acs.org.

Author Information

- Corresponding Author
    - H. V. Rasika Dias - Department of Chemistry and Biochemistry, The University of Texas at Arlington, Arlington, Texas 76019, United States; https://orcid.org/0000-0002-2362-1331; Email: dias@uta.edu
- Authors
    - Mukundam Vanga - Department of Chemistry and Biochemistry, The University of Texas at Arlington, Arlington, Texas 76019, United States; https://orcid.org/0000-0002-7822-4181
    - Vo Quang Huy Phan - Department of Chemistry and Biochemistry, The University of Texas at Arlington, Arlington, Texas 76019, United States; https://orcid.org/0009-0004-3436-4168
    - Jiang Wu - Department of Chemistry and Biochemistry, The University of Texas at Arlington, Arlington, Texas 76019, United States
    - Alvaro Muñoz-Castro - Facultad de Ingeniería, Arquitectura y Diseño, Universidad San Sebastián, Bellavista 7, Santiago, 8420524, Chile.

- Author Contributions

  The manuscript was written through contributions of all authors. All authors have given approval to the final version of the manuscript.

- Notes

  The authors declare no competing financial interest.

Acknowledgments

This material is based upon work supported by the National Science Foundation under grant number (CHE-1954456, HVRD). A.M.-C thanks support from ANID FONDECYT Regular 1221676. We thank Dr. Brian Edwards for his assistance with the VT NMR spectroscopic data collection.

References:

1. Trofimenko, S., Recent advances in poly(pyrazolyl)borate (scorpionate) chemistry. *Chem. Rev.* **1993,** *93* (3), 943-80. DOI: 10.1021/cr00019a006.

2. Pettinari, C.; Santini, C., Polypyrazolylborate and scorpionate ligands. McCleverty, J. A.; Meyer, T. J., Eds. Elsevier: Oxford, 2004; Vol. 1, pp 159-210.

3. Trofimenko, S., *Scorpionates - The Coordination Chemistry of Polypyrazolylborate Ligands*. Imprerial College Press: London, 1999.

4. Pettinari, C., *Scorpionates II: Chelating Borate Ligands*. Imperial College Press: London, 2008.

5. Santini, C.; Pellei, M.; Lobbia, G. G.; Papini, G., Synthesis and properties of poly (pyrazolyl) borate and related boron-centered scorpionate ligands. Part A: Pyrazole-based systems. *Mini-Rev. Org. Chem.* **2010,** *7* (2), 84-124.

6. Fischer, P. J., 1.14 - Polypyrazolylborates and Scorpionates. In *Comprehensive Coordination Chemistry III*, Constable, E. C.; Parkin, G.; Que Jr, L., Eds. Elsevier: Oxford, 2021; pp 428-504.

7. Pettinari, C.; Pettinari, R.; Marchetti, F., Chapter Four - Golden Jubilee for Scorpionates: Recent Advances in Organometallic Chemistry and Their Role in Catalysis. In *Advances in Organometallic Chemistry*, Pérez, P. J., Ed. Academic Press: 2016; Vol. 65, pp 175-260.

8. Dias, H. V. R.; Lovely, C. J., Carbonyl and Olefin Adducts of Coinage Metals Supported by Poly(pyrazolyl)borate and Poly(pyrazolyl)alkane Ligands and Silver Mediated Atom Transfer Reactions. *Chem. Rev.* **2008,** *108* (8), 3223-3238. DOI: 10.1021/cr078362d.

9. Janiak, C., Hydrotris(pyrazolyl)borate thallium(I) [TpTl(I)] chemistry syntheses and applications. *Main Group Met. Chem.* **1998,** *21* (1), 33-49. DOI: 10.1515/mgmc.1998.21.1.33.

10. Dias, H. V. R., Indium and thallium. In *Comprehensive Coordination Chemistry II; From Biology to Nanotechnology*, Constable, E.; McCleverty, J. A.; Meyer, T. J., Eds. Elsevier Science: 2004; Vol. 3, pp 383-463.

11. Fischer, P. J.; Roe, C. B.; Stephenson, J. N.; Dunscomb, R. J.; Carthy, C. L.; Nataro, C.; Young, V. G., Exploring opportunities for tuning phenyltris(pyrazol-1-yl)borate donation by varying the extent of phenyl substituent fluorination. *Dalton Trans.* **2023,** *52* (17), 5606-5615. DOI: 10.1039/D3DT00735A.

12. Dias, H. V. R.; Wang, X., Sterically demanding methyltris(pyrazolyl)borate ligands: synthesis and characterization of thallium(I) complexes supported by $[MeB(3\text{-}(t\text{-}Bu)Pz)_3]^-$ and $[MeB(3\text{-}(Mes)Pz)_3]^-$. *Polyhedron* **2004,** *23* (16), 2533-2539. DOI: 10.1016/j.poly.2004.08.023.

13. Dias, H. V. R.; Huai, L.; Jin, W.; Bott, S. G., Synthesis and Chemistry of [Hydridotris(3-t-butylpyrazolyl)borato]indium(I). *Inorg. Chem.* **1995,** *34* (8), 1973-4. DOI: 10.1021/ic00112a001.

14. Janiak, C., (Organo)thallium (I) and (II) chemistry: Syntheses, structures, properties and applications of subvalent thallium complexes with alkyl, cyclopentadienyl, arene or hydrotris(pyrazolyl)borate ligands. *Coord. Chem. Rev.* **1997,** *163*, 107-216. DOI: https://doi.org/10.1016/S0010-8545(97)00011-8.

15. Kitamura, M.; Takenaka, Y.; Okuno, T.; Holl, R.; Wunsch, B., A new, efficient and direct preparation of TlTp and related complexes with $TlBH_4$. *Eur. J. Inorg. Chem.* **2008,** (8), 1188-1192. DOI: 10.1002/ejic.200701366.

16. Rheingold, A. L.; Liable-Sands, L. M.; Trofimenko, S., Formation of a tetrahedral Tl_4 cluster directed by a novel homoscorpionate ligand. *Chem. Commun.* **1997,** (17), 1691-1692. DOI: 10.1039/a703349d.

17. Sirianni, E. R.; Yap, G. P. A.; Theopold, K. H., Ferrocenyl-Substituted Tris(pyrazolyl)borates-A New Ligand Type Combining Redox Activity with Resistance to Hydrogen Atom Abstraction. *Inorg. Chem.* **2014,** *53* (17), 9424-9430. DOI: 10.1021/ic5015658.

18. Ghosh, P.; Desrosiers, P. J.; Parkin, G., Chemical Shift Anisotropy as a Mechanism for Modulating Apparent $J_{Tl\text{-}H}$ and $J_{Tl\text{-}C}$ Coupling Constants in Tris(pyrazolyl)hydroborato Thallium Complexes. *J. Am. Chem. Soc.* **1998,** *120* (40), 10416-10422. DOI: 10.1021/ja981636h.

19. Han, R.; Ghosh, P.; Desrosiers, P. J.; Trofimenko, S.; Parkin, G., Synthesis and structural characterization of tris[3-trifluoromethyl-5-(2-thienyl)pyrazolyl]hydroborato thallium, Tl[$Tp^{CF3,Tn}$]: a monovalent thallium complex with a highly solvent dependent J_{Tl-F} coupling constant, ranging from 0 to 850 Hz. *J. Chem. Soc., Dalton Trans.* **1997,** (20), 3713-3717.

20. McQuade, J.; Jakle, F., Tris(pyridyl)borates: an emergent class of versatile and robust polydentate ligands for catalysis and materials applications. *Dalton Trans.* **2023,** *52*, 10278-10285 DOI: 10.1039/d3dt01665j.

21. Vanga, M.; Munoz-Castro, A.; Dias, H. V. R., Fluorinated tris(pyridyl)borate ligand support on coinage metals. *Dalton Trans.* **2022,** *51* (4), 1308-1312. DOI: 10.1039/d1dt04136c.

22. Vanga, M.; Noonikara-Poyil, A.; Wu, J.; Dias, H. V. R., Carbonyl and Isocyanide Complexes of Copper and Silver Supported by Fluorinated Poly(pyridyl)borates. *Organometallics* **2022,** *41* (10), 1249-1260. DOI: 10.1021/acs.organomet.2c00134.

23. Watson, B. T.; Vanga, M.; Noonikara-Poyil, A.; Munoz-Castro, A.; Dias, H. V. R., Copper(I), Silver(I), and Gold(I) Ethylene Complexes of Fluorinated and Boron-Methylated Bis- and Tris(pyridyl)borate Chelators. *Inorg. Chem.* **2023,** *62* (4), 1636-1648. DOI: 10.1021/acs.inorgchem.2c04009.

24. Qian, J.; Comito, R. J., Site-Isolated Main-Group Tris(2-pyridyl)borate Complexes by Pyridine Substitution and Their Ring-Opening Polymerization Catalysis. *Inorg. Chem.* **2022,** *61* (28), 10852-10862. DOI: 10.1021/acs.inorgchem.2c01289.

25. Cui, C.; Lalancette, R. A.; Jäkle, F., The elusive tripodal tris(2-pyridyl)borate ligand: a strongly coordinating tetraarylborate. *Chem. Commun.* **2012,** *48* (55), 6930-6932. DOI: 10.1039/C2CC33059H.

26. Fujiwara, Y.; Takayama, T.; Nakazawa, J.; Okamura, M.; Hikichi, S., Development of a novel scorpionate ligand with 6-methylpyridine and comparison of the structural and electronic properties of nickel(II) complexes with related tris(azolyl)borates. *Dalton Trans.* **2022,** *51* (27), 10338-10342. DOI: 10.1039/d2dt01548j.

27. Groom, C. R.; Bruno, I. J.; Lightfoot, M. P.; Ward, S. C., The Cambridge Structural Database. *Acta Cryst. B* **2016,** *72* (2), 171-179. DOI: doi:10.1107/S2052520616003954.

28. Renn, O.; Vananzi, L. M.; Marteletti, A.; Gramlich, V., High-yield syntheses of sodium, potassium, and thallium hydrotris[3,5-bis(trifluoromethyl)pyrazolyl]borates and the x-ray crystal structure of {hydrotris[3,5-bis(trifluoromethyl)pyrazolyl]borato}thallium(I). *Helv. Chim. Acta* **1995,** *78* (4), 993-1000. DOI: 10.1002/hlca.19950780420.

29. Dias, H. V. R.; Thankamani, J., Thallium(I) complexes of fluorinated bis- and tris(pyrazolyl)borate ligands: $[H_2B\{3,5\text{-}(CF_3)_2pz\}_2]Tl$ and $[HB\{3,5\text{-}(CF_3)_2pz\}_3]Tl$. *Acta Crystallogr., Sect. C Cryst. Struct. Commun.* **2013,** *69* (9), 959-962. DOI: 10.1107/s0108270113016612.

30. Dias, H. V. R.; Wang, X.; Diyabalanage, H. V. K., Fluorinated Tris(pyrazolyl)borate Ligands without the Problematic Hydride Moiety: Isolation of Copper(I) Ethylene and Copper(I)-Tin(II) Complexes Using $[MeB(3\text{-}(CF_3)Pz)_3]^-$. *Inorg. Chem.* **2005,** *44* (21), 7322-7324. DOI: 10.1021/ic0513235.

31. Ojo, W.-S.; Jacob, K.; Despagnet-Ayoub, E.; Munoz, B. K.; Gonell, S.; Vendier, L.; Nguyen, V.-H.; Etienne, M., Highly Fluorinated Aryl-Substituted Tris(indazolyl)borate Thallium Complexes: Diverse Regiochemistry at the B-N Bond. *Inorg. Chem.* **2012,** *51* (5), 2893-2901. DOI: 10.1021/ic202125c.

32. Despagnet-Ayoub, E.; Jacob, K.; Vendier, L.; Etienne, M.; Alvarez, E.; Caballero, A.; Diaz-Requejo, M. M.; Perez, P. J., A New Perfluorinated F_{21}-Tp Scorpionate Ligand: Enhanced Alkane Functionalization by Carbene Insertion with (F_{21}-Tp)M Catalysts (M = Cu, Ag). *Organometallics* **2008,** *27* (18), 4779-4787. DOI: 10.1021/om800531a.

33. Gava, R.; Olmos, A.; Noverges, B.; Varea, T.; Alvarez, E.; Belderrain, T. R.; Caballero, A.; Asensio, G.; Perez, P. J., Discovering Copper for Methane C-H Bond Functionalization. *ACS Catal.* **2015,** *5* (6), 3726-3730. DOI: 10.1021/acscatal.5b00718.

34. Dias, H. V. R.; Goh, T. K. H. H., Tris(3-trifluoromethyl,5-phenylpyrazolyl)hydroborato thallium(I). *CSD Communication* **2023**, DOI: 10.5517/ccdc.csd.cc2grpb8; CCDC Number: 2286880.

35. Bondi, A., van der Waals Volumes and Radii. *J. Phys. Chem.* **1964,** *68* (3), 441-451. DOI: 10.1021/j100785a001.

36. Allan, C. J.; MacDonald, C. L. B., Low-Coordinate Main Group Compounds - Group 13. *Comprehensive Inorganic Chemistry II (Second Edition): From Elements to Applications* **2013,** *1*, 485-566. DOI: 10.1016/B978-0-08-097774-4.00121-2.

37. Cordero, B.; Gómez, V.; Platero-Prats, A. E.; Revés, M.; Echeverría, J.; Cremades, E.; Barragán, F.; Alvarez, S., Covalent radii revisited. *Dalton Trans.* **2008,** (21), 2832-2838. DOI: 10.1039/B801115J.

38. Falivene, L.; Cao, Z.; Petta, A.; Serra, L.; Poater, A.; Oliva, R.; Scarano, V.; Cavallo, L., Towards the online computer-aided design of catalytic pockets. *Nat. Chem.* **2019,** *11* (10), 872-879. DOI: 10.1038/s41557-019-0319-5.

39. Gómez-Suárez, A.; Nelson, D. J.; Nolan, S. P., Quantifying and understanding the steric properties of N-heterocyclic carbenes. *Chem. Commun.* **2017,** *53* (18), 2650-2660. DOI: 10.1039/C7CC00255F.

40. Fujisawa, K.; Takisawa, H., {Tris[3-(adamantan-1-yl)-5-isopropylpyrazol-1-yl-[*k*N_2]hydroborato}thallium(I): the scorpionate with the most bulk? *Acta Cryst. C* **2013,** *69* (9), 986-989. DOI: doi:10.1107/S0108270113021677.

41. Fujisawa, K.; Shimizu, D.; Tiekink, E. R. T., Crystal structure of {hydridotris[3-(*t*-butyl)-5-isopropylpyrazol-1-yl-κN_3]borato}thallium(I), $C_{30}H_{52}BN_6Tl$. *Z. Kristallogr. - New Cryst. Struct.* **2021,** *236* (1), 169-172. DOI: doi:10.1515/ncrs-2020-0405.

42. Thallium exists as two naturally occurring spin 1/2 isotopes ^{203}Tl (29.5%) and ^{205}Tl (70.5%). However, due to the similarity of their gyromagnetic ratios, the difference in ^{203}Tl and ^{205}Tl coupling constants is generally not noticeable.

43. Hinton, J. F., Thallium NMR spectroscopy. *Magn. Reson. Chem.* **1987,** *25* (8), 659-669. DOI: https://doi.org/10.1002/mrc.1260250802.

44. Bakar, W. A. W. A.; Davidson, J. L.; Lindsell, W. E.; McCullough, K. J.; Muir, K. W., Monocyclopentadienyl pentafluorothiophenolate complexes of molybdenum and their interactions with

thallium(I) ions; dynamic nuclear magnetic resonance studies and crystal and molecular structures of [TlMo(SC_6F_5)$_2$$L_2$(cp)](L = CO or SC_6F_5; cp = η^5-C_5H_5). *J. Chem. Soc., Dalton Trans.* **1989,** (5), 991-1001. DOI: 10.1039/DT9890000991.

45. Bakar, W. A. W. A.; Davidson, J. L.; Lindsell, W. E.; McCullough, K. J.; Muir, K. W., Cyclopentadienyl pentafluorophenylthiolate complexes of molybdenum and tungsten as novel polydentate ligands of thallium(I); dynamic NMR studies and crystal structures of two derivatives [MoTl(SC_6F_5)$_2$$L_2$Cp] (L = SC_6F_5 or CO). *J. Organomet. Chem.* **1987,** *322* (1), C1-C6. DOI: https://doi.org/10.1016/0022-328X(87)85032-5.

46. Alvarez, S., A cartography of the van der Waals territories. *Dalton Trans.* **2013,** *42* (24), 8617-8636. DOI: 10.1039/C3DT50599E.

47. Lee, H. S.; Hauber, S.-O.; Vinduš, D.; Niemeyer, M., Isostructural Potassium and Thallium Salts of Sterically Crowded Triazenes: A Structural and Computational Study. *Inorg. Chem.* **2008,** *47* (10), 4401-4412. DOI: 10.1021/ic800029z.

48. Sarazin, Y.; Hughes, D. L.; Kaltsoyannis, N.; Wright, J. A.; Bochmann, M., Thallium(I) Sandwich, Multidecker, and Ether Complexes Stabilized by Weakly-Coordinating Anions: A Spectroscopic, Structural, and Theoretical Investigation. *J. Am. Chem. Soc.* **2007,** *129* (4), 881-894. DOI: 10.1021/ja0657105.

49. Dias, H. V. R.; Singh, S.; Cundari, T. R., Monomeric thallium(I) complexes of fluorinated triazapentadienyl ligands. *Angew. Chem., Int. Ed.* **2005,** *44* (31), 4907-4910. DOI: 10.1002/anie.200500401.

50. Kunz, K.; Blasberg, F.; Bolte, M.; Lerner, H.-W.; Wagner, M., Synthesis and structural characterisation of the phenyl/scorpionate hybrid ligand $[Ph(pz)BC_5H_{10}]^-$. *Inorg. Chim. Acta* **2009,** *362* (12), 4372-4376. DOI: https://doi.org/10.1016/j.ica.2009.02.002.

51. Kisko, J. L.; Hascall, T.; Kimblin, C.; Parkin, G., Phenyl tris(3-tert-butylpyrazolyl)borato complexes of lithium and thallium, [PhTpBu^t]M (M = Li, Tl): a novel structure for a monomeric

tris(pyrazolyl)boratothallium complex and a study of its stereochemical nonrigidity by ^{1}H and ^{205}Tl NMR spectroscopy. *J. Chem. Soc., Dalton Trans.* **1999,** (12), 1929-1936.

52. Dias, H. V. R.; Wu, J., Structurally Characterized Coinage-Metal–Ethylene Complexes. *Eur. J. Inorg. Chem.* **2008,** *2008* (4), 509-522. DOI: https://doi.org/10.1002/ejic.200701055.

53. Dias, H. V. R.; Wu, J., Structurally Similar, Thermally Stable Copper(I), Silver(I), and Gold(I) Ethylene Complexes Supported by a Fluorinated Scorpionate. *Organometallics* **2012,** *31* (4), 1511-1517. DOI: 10.1021/om201185v.

54. Lik, A.; Fritze, L.; Müller, L.; Helten, H., Catalytic B–C Coupling by Si/B Exchange: A Versatile Route to π-Conjugated Organoborane Molecules, Oligomers, and Polymers. *J. Am. Chem. Soc.* **2017,** *139* (16), 5692-5695. DOI: 10.1021/jacs.7b01835.

55. Flores, D. M.; Schmidt, V. A., Intermolecular 2 + 2 Carbonyl–Olefin Photocycloadditions Enabled by Cu(I)–Norbornene MLCT. *J. Am. Chem. Soc.* **2019,** *141* (22), 8741-8745. DOI: 10.1021/jacs.9b03775.

56. Krause, L.; Herbst-Irmer, R.; Sheldrick, G. M.; Stalke, D., Comparison of silver and molybdenum microfocus X-ray sources for single-crystal structure determination. *J. Appl. Crystallogr.* **2015,** *48* (1), 3-10. DOI: doi:10.1107/S1600576714022985.

57. Sheldrick, G., SHELXT - Integrated space-group and crystal-structure determination. *Acta Crystallogr. Sect. A: Found. Adv.* **2015,** *71* (1), 3-8. DOI: doi:10.1107/S2053273314026370.

58. Sheldrick, G., Crystal structure refinement with SHELXL. *Acta Crystallogr. Sect. C: Struct. Chem.* **2015,** *71* (1), 3-8. DOI: doi:10.1107/S2053229614024218.

59. Dolomanov, O. V.; Bourhis, L. J.; Gildea, R. J.; Howard, J. A. K.; Puschmann, H., OLEX2: a complete structure solution, refinement and analysis program. *J. Appl. Crystallogr.* **2009,** *42* (2), 339-341. DOI: 10.1107/s0021889808042726.